Journal of Mining and Geology Vol. 58(2) 2022. pp. 95 - 113 0022-2763
© Nigerian Mining and Geosciences Society (NMGS) - Printed in Nigeria.

Sedimentary Geochemistry of Campanian-Maastrichtian sandstones at the Agbaja Plateau, southern Bida Basin, Nigeria: Implications for provenance, paleotectonics and palaeoenvironmental reconstruction

Awe, A.[1], Ojo, O.J.[1] and Adepoju, S.A.[2]
[1]Department of Geology, Federal University, Oye-Ekiti, Nigeria.
[2]Department of Geology and Mineral Sciences, Kwara State University, Malete, Nigeria
Corresponding E-mail: **ayodeji.awe@fuoye.edu.ng**

Abstract
The sandstones in the Bida Basin exposed at Agbaja Plateau were profiled and sampled. The samples were analyzed for major, trace and rare earth elements. The study aims to provide insight into the Late Cretaceous palaeogeography within the context of geochemical proxies. The results show that the sandstones are of felsic origin and deposited in passive margin setting. The palaeoclimatic condition varied with less humidity in the early history of the basin (Campanian) but warmer and more humid later in the Maastrichtian. The sandstones in the upper part of the section are intensively weathered with more pervasive weathering in the Maastrichtian sandstones compared to the basal Campanian sandstones. The scenario is interpreted to be reflective of more humidity and marine incursion from both the Tethys Sea and the South Atlantic Ocean. Generally, the sandstones units were deposited dominantly in oxic setting with the older sandstone showing more oxic condition than the younger sandstones which may be responsible for improved paleoproductivity in the younger sandstones. The sandstones units are characterized by dominant marine organic matter diluted by high continental detritus. The transition from basal arkosic sandstone to upper arenitic sandstone is marked by low temperature regime at Campanian-Maastrichtian boundary. The study revealed that the southern Bida Basin belongs to the West Africa Rift System that was probably inundated by Tethys Sea and south Atlantic Ocean in the Late Cretaceous.

Keywords: *Paleoproductivity, paleosalinity, provenance, paleotectonics*

Introduction

The Bida Basin is an intracratonic sedimentary basin located in the central part of Nigeria (Fig. 1) . It is a NW-SE trough that is bordered in NW by Sokoto Basin and SE by the Anambra Basin. The palaeoenvironmental reconstruction is pivotal to basin analysis as it gives insight into past geological and climatic conditions under which the sediments were deposited. The sedimentary geochemistry as a tool has been widely applied in unravelling the geological history of sedimentary basins across the world. Sarki Yandoka et al. (2015) and Omietimi et al. (2022) used inorganic geochemistry to unravel the palaeoenvironmental conditions of Yola sub-basin and Anambra Basin respectively in Nigeria. Since the stratigraphy of the Anambra Basin has been correlated with the Bida Basin by Akande et al. (2005) using facies characteristics, it is possible the two basins share similar palaeoenvironmental history. The sedimentary geochemistry of the Bida Basin is used in this work to unravel the provenance, palaeotectonic setting and palaeoenvironmental conditions of the basin. Previous studies revealed that abundances and ratios of some trace elements can be used to probe sedimentation history and palaeoenvironmental condition (Jones and Manning, 1994; Song et al., 2012; Bai et al., 2015) . Elements including rare-earth element (REE) , Sc, La, Th, and Co are less mobile. Hence, they are likely well preserved in the clastic sediments during sedimentation processes. These elements are thereby useful to infer the provenance composition (McLennan et al., 1993; Armstrong-Altrin et al., 2014; Bai et al., 2015) .Song et al. (2018) used geochemistry to determine provenance, diagenetic imprint and palaeoclimatic history of siliciclastic sediments. Chang et al. (2013) used Rb/Sr for palaeoenvironmental deduction and palaeotectonic of Tarim Basin.The varying properties of Rb and Sr in geological processes are useful in determining the provenance and chemical weathering intensity (Chen et al., 2000; Xu et al., 2010) as Sr, just as Ca, is more reactive than Rb. Chang et al. (2013) reported that the Rb/Sr ratio of sediments is largely determined by the source which may also rely on the climate. Convers (2020) used major element and their proxies to predict the nutrient quality of sediment and palaeoclimatic condition in the early Cenozoic. The study predicted multiple dynamic global warming events.Chen et al. (2021) also reported that the weathering intensity of sediments can be greatly influenced by grain size and source rock.

Climate controls several environmental factors such as rainfall which determines palaeoproductivity, sea level, detritus influx and salinity. Calvert et al. (1992) suggested that organic matter preservation depends on

sediment deposition rate, water depth, and paleoredox conditions. Sea-level variation, which is a function of climatic condition, mostly control water redox conditions and organic productivity (Werneet al., 2002) . Previous studies revealed that sea-level rise enhances supply of water nutrients which may spike marine productivity via emerging anoxic condition (Rohlet al., 2001; Frimmel et al., 2004) . The tendency of organic matter preservation is also dependent on the paleoredox condition. Song et al. (2018) also reported that a hot and very dry climate involves a relatively low rainfall which may result in overall lower lake-level and higher palaeosalinity. They suggested that saline sedimentary environment may inhibit the survival of microflora and microfauna which may result in low palaeoproductivity. A warm–humid palaeoclimate condition might increase the rainfall and melting of polar region thereby leading to increase in palaeowater which may increase the terrigenous nutritional minerals supply and microbial boom.

Prior to this present study, fossils have been the only source of palaeoenvironmental deduction in the Bida Basin and the studies have been restricted to only the argillaceous rocks (Jan du Chene et al., 1978; Mebradu et al., 1986; Agyingi, 1993; Ojo and Akande, 2006; 2008; Ojo, 2010; Ojo and Akande, 2012) . Compared with the sandstone facies which are wide spread in the basin, the argillaceous rocks are limited both in space and time and therefore, the palaeogeographic deductions reported may not be representative enough. Hence, there is need to have a wider knowledge of the palaeoenvironmental conditions such as palaeosalinity, palaeobathymetry, palaeohydrodynamics, palaeoproductivity, detrital influx and palaeoclimate from the non-fossiliferous but widely distributed sandstones in the Bida Basin. This work focusses on detail palaeoenvironmental studies via sedimentary geochemistry of sandstone facies which make up more than 70% of the Bida Basin stratigraphy.

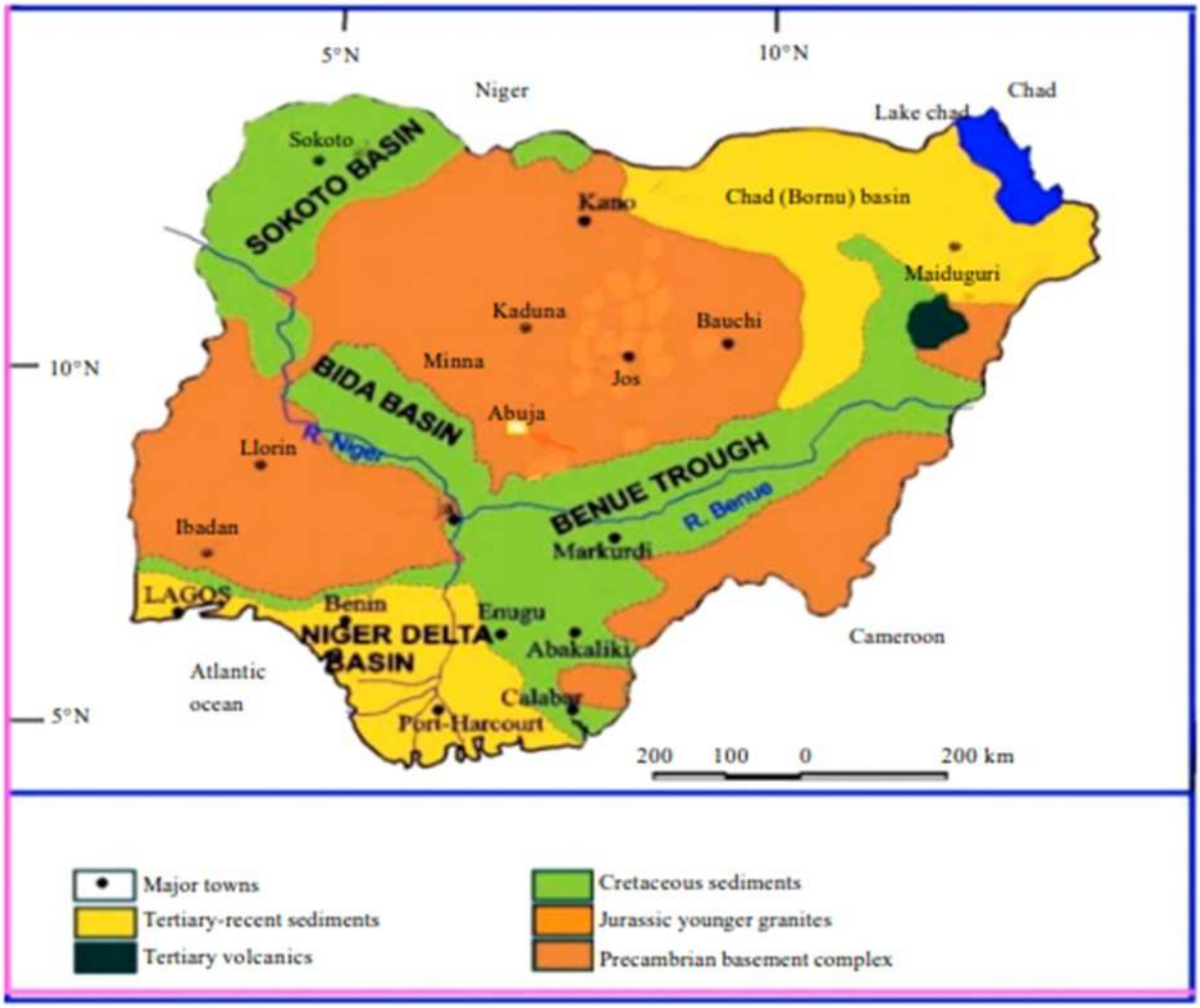


Fig. 1: Generalized geological map of Nigeria with emphasis on the Bida Basin (adapted from Adegoke and Layade, 2014; Obaje, 2009)

Geological Setting of the Bida Basin

The evolution of the Bida Basin is linked to the emergence of the south Atlantic Ocean sequel to fragmentation of the Pangea and subsequent drifting apart of the African and south American plates. The Bida Basin is a rift basin that originated from faulting associated with the Benue Trough System and drifting apart of the African and Brazilian plates in the Cretaceous (King, 1950; Kennedy, 1965; Salawu et al., 2021) . Kogbe et al. (1983) reported that the southern Bida Basin is dominated by NW-SE trending faults which support a rift model for the basin. This is corroborated by Ojo and Ajakaiye (1989) . However, Braide (1992) suggested a wrench fault or strike-slip tectonic model for the basin. The basin comprises about 3.5km thick of sediments (Udensi and Osazuwa, 2004) . The stratigraphy of the Bida Basin has been described by several authors (Jones, 1958; Adeleye and Dessauvagie, 1972; Idowu and Enu, 1992; Agyingi, 1991; 1993; Akande et al., 2005, Rahaman et al., 2019; Ojo and Akande, 2020) . The stratigraphy in southern part of the basin comprises of basal Lokoja Formation which comprises conglomerate, sandstone and claystone. The Lokoja Formation is overlain by Patti Formation which comprises dominantly sandstone and other lithologies which include siltstone, shale, claystone, concretional ironstone and lignite. The sequence in capped by ironstone facies which is described as Agbaja Formation. In the northern Bida Basin, the basal formation is Bida Formation, which is the stratigraphic equivalent of Lokoja Formation. The Bida Formation comprises conglomerate, sandstone and claystone members. This is overlain by Sakpe Formation which is contains mainly ironstone facies. The Sakpe Formation is overlain by Enagi Formation which is stratigraphic equivalent of Patti Formation. The Enagi Formation comprises sandstone, siltstone and claystone. The northern sub-basin stratigraphy is capped by ironstone facies referred to as Batati Formation (Fig. 2).

Materials and Methods

The Agbaja Plateau cliff face provides an excellent representation of southern Bida Basin stratigraphy. The section was compositely logged from base to the top through road cuts, taking cognizance of lithology, texture, mineralogy and sedimentary structures. The fresh and representative sandstones were sampled up-section. Nine selected samples of the sandstones were analyzed for bulk elemental composition; major oxides, trace elements and REEs using both X-ray Fluorescence

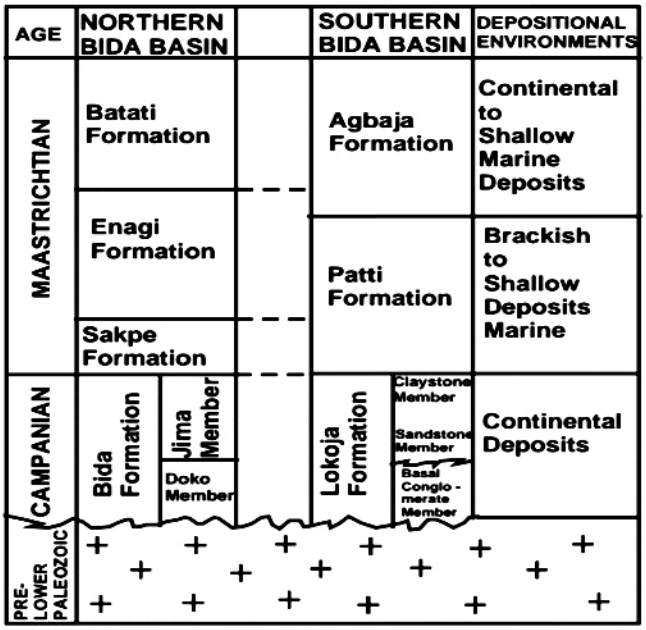


Fig. 2: Lithostratigraphic successions of the Bida Basin (Ojo and Akande, 2009)

(XRF) and aqua regia ultra-trace Inductively Coupled Plasma Mass Spectroscopy (ICP-MS) analyses which were carried out at MS Analytical Laboratory, Canada. The samples selected for XRF analysis were pulverized to 85% passing 200mesh (75µm) in a mild-steel ring-and-puck mill following the dryness at 60° C followed by pulverization via a jaw crusher to 70% passing a 10 mesh (2 mm) . A 0.2 g aliquot was weighed into a graphite crucible and mixed with 1.5 g of $LiBO_2/Li_2B_4O_7$ flux. The crucibles were heated in a 980° C oven for 30 min. The resulting bead was dissolved in 5% HNO_3 (ACS grade nitric acid diluted in dematerialized water) . Samples and calibration reagent blanks were aspirated into an XRF (SpectroCiros Vision or Varian 735) to determine the set of major oxides and elements. Loss on ignition (LOI) was determined by igniting a 1.0 g sample split at 950° C for 90 min, then measuring the weight loss. Samples for ICP-MS analysis were pulverized to 95% passing 150mesh (100µm) in a mild-steel ring-and-puck mill. A 0.2 g aliquot was weighed into a graphite crucible and mixed with 1.5 g of $LiBO_2/Li_2B_4O_7$ flux. The crucibles were heated in a 980° C oven for 30 minutes. The resulting bead was dissolved in 100 mL 5% HNO_3 (ACS grade nitric acid diluted in demineralized water) . An aliquot of the solution was poured into a polypropylene test tube. Samples and calibrated reagent blanks were aspirated into an ICP-MS (PerkinElmer Elan 6000 or 9000) and a digested split of 0.5 g in Aqua Regia aspirated into an ICP-MS to determine the suite of major elements, trace elements and rare earth elements.

Results and Discussion

Lithological Description

The composite lithologic profile is shown in Fig. 3. The entire sedimentary sequence of Agbaja Plateau is dominated byfining upward sequences. The basal conglomerate and sandstone units (beds A-E) are slightly feldspathic, massive and dominantly poorly sorted. The upper part (sandstone beds F-Y) is less feldspathic, dominantly fine to medium grained sandstones with siltstone and claystone interbeds. These sandstones are moderately to well sorted. The entire section is capped with oolitic ironstone.

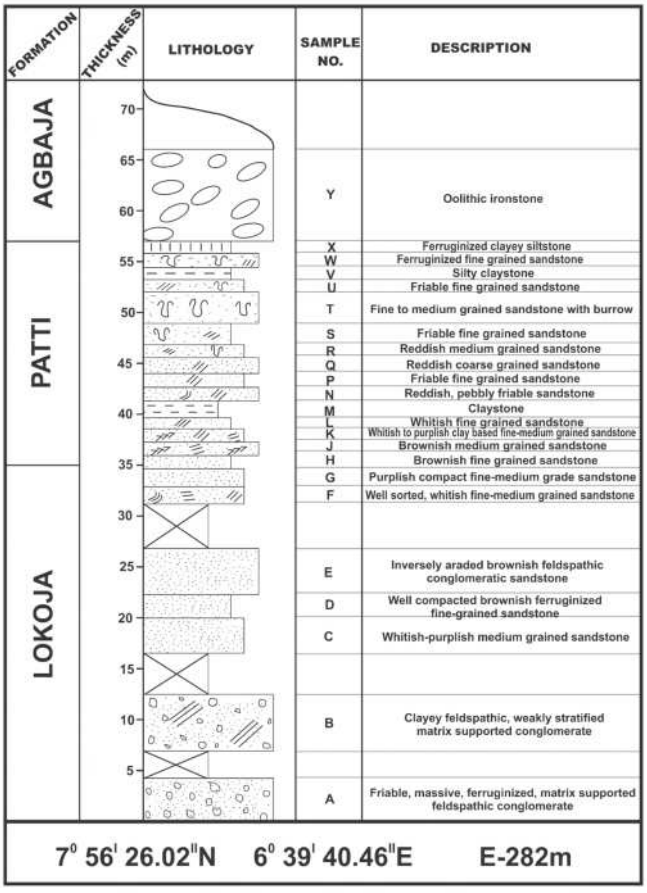


Fig. 3: Litholog of the Agbaja Plateau section showing rock successions from the base to the top

Geochemistry

The major, trace and rare earth elemental data of Agbaja Plateau sandstones is shown in Tables 1-3 while the calculated values of geochemical proxies are shown in Table 4. The graphical representation of the geochemical data is shown in figures 4a-c. The three major oxides in the sandstones are SiO_2 (73.3% to 97.49%) , Al_2O_3 (1.41% to 15.75%) and Fe_2O_3 (1.51% to 6.31%) . The alumina content of the sandstones also reduces up the section. In sandstone beds AA – AL, alumina content varies from 9.4% to 15.75%. while from AQ to AW, their alumina ranges from 0.73% to 2.02%. The Fe_2O_3 content across the section is relatively stable and low, ranging from 1.51% to 6.31%. The SiO_2 content of the sandstone at the lower part of the section varies from 73.3% to 82.69%) while the sandstone at the upper part of the section are more enriched in SiO_2 (92.06% to 97.49%) . When compared and normalized to PAAS data of Taylor and McLennan (1985) , the trace elements concentrations and REE concentration are generally low. There is 38.1ppm Molybdenum (Mo) spike at the uppermost bed. The sandstones are enriched in SiO_2, Al_2O_3, Fe_2O_3 and TiO_2 while they are depleted in Na_2O, K_2O, MgO and CaO. The depleted oxides indicate probable high intensity of weathering. Also, feldspar-related trace elements such as Ba, Rb, Sr are dominant in the lower part of the section. They are also depleted in Ni, Zn, Cu, Ce, Nd and Sm while they are enriched in Cr, Zr, Th, U, Nb, Yb, La, Eu, Gd, Dy and Er (Figs. 5 to 7).

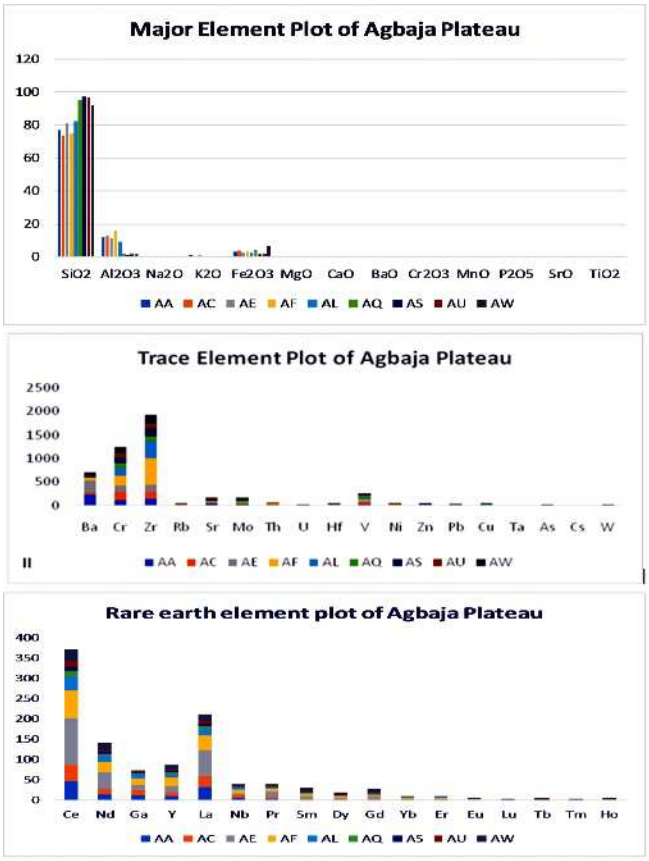


Fig. 4: (I) – Histogram showing major element distribution in Agbaja Plateau sandstones (II) – Composite bar chart showing trace element distribution in Agbaja Plateau sandstone (III) Composite bar chart showing rare earth element distribution in Agbaja Plateau sandstones.

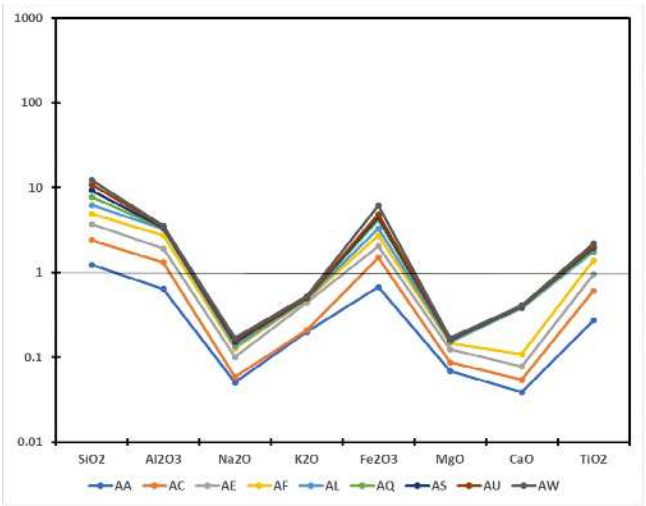


Fig. 5: Plot of major element oxides normalized to PAAS of Taylor and McLennan (1985) showing depletion in Na_2O, K_2O, MgO and CaO.

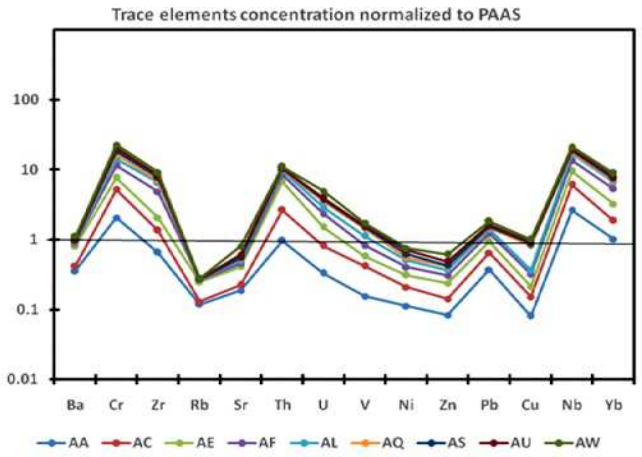


Fig. 6: Plot of trace elements normalized to PAAS of Taylor and McLennan (1985) showing depletion in Rb and St which are mostly associated with feldspar. There is also depletion in Zn and Cu.

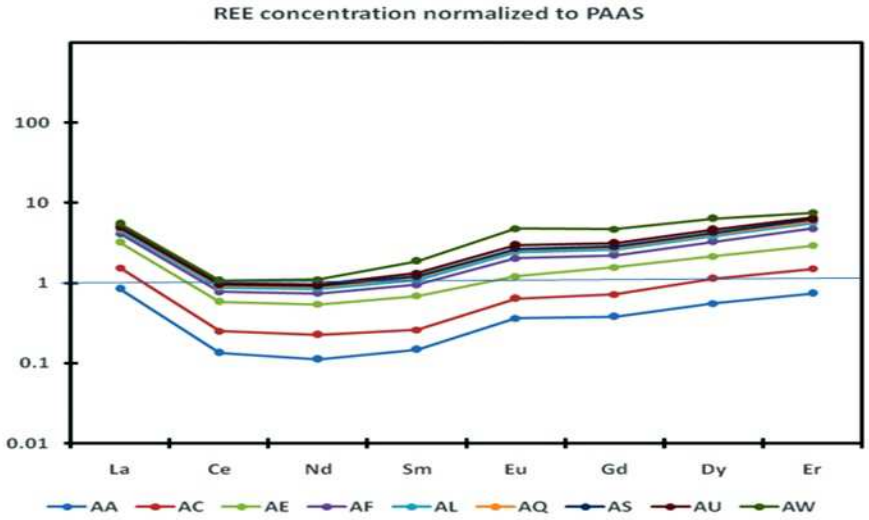


Fig. 7: Plot of rare earth elements normalized to PAAS of Taylor and McLennan (1985) showing negative anomaly for Ce and Nd.

Table 1: Major element data of Agbaja Plateau sandstones (AA is sample from bed A, AC is sample from bed C and so on.

	AA	AC	AE	AF	AL	AQ	AS	AU	AW	MEAN	PAAS
SiO_2	76.74	73.3	80.74	75.09	82.69	95.57	97.49	96.76	92.06	85.60444	62.4
Al_2O_3	12.02	12.61	11.17	15.75	9.4	1.41	0.73	2.02	1.52	7.403333	18.78
Na_2O	0.06	0.01	0.05	0.03	0.01	0.01	0.01	0.01	0.01	0.022222	1.19
K_2O	0.73	0.04	0.84	0.14	0.02	0.03	0.03	0.03	0.07	0.214444	3.68
Fe_2O_3	3.18	3.9	2.6	3.22	2.67	4.14	1.58	1.51	6.31	3.234444	4.72
MgO	0.15	0.04	0.08	0.05	0.01	0.01	0.01	0.01	0.01	0.041111	2.19
CaO	0.05	0.02	0.03	0.04	0.35	0.01	0.01	0.01	0.01	0.058889	1.29
BaO	0.03	0.01	0.03	0.01	0.01	0.01	0.01	0.01	0.01	0.014444	nil
Cr_2O_3	0.02	0.02	0.02	0.03	0.02	0.02	0.02	0.01	0.02	0.02	nil
MnO	0.01	0.01	0.01	0.02	0.01	0.01	0.01	0.01	0.01	0.011111	nil
P_2O_5	0.01	0.01	0.02	0.01	0.02	0.05	0.01	0.01	0.1	0.026667	nil
SrO	0.01	0.01	0.01	0.01	0.01	0.01	0.01	0.01	0.01	0.01	nil
TiO_2	0.27	0.33	0.34	0.43	0.36	0.09	0.11	0.08	0.16	0.241111	0.99
LOI	6.35	5.53	5.21	6.47	3.72	0.59	0.13	0.72	1.03	3.305556	nil
Total	99.59	95.82	101.15	101.27	99.25	101.9	100.1	101.15	101.29	100.2078	95.24

Table 2: Trace elements data of Agbaja Plateau sandstones

	AA	AC	AE	AF	AL	AQ	AS	AU	AW	MEAN	PAAS
Ba	230.3	40.9	248.4	58.7	23.5	12.5	8	20.1	63.7	78.45556	650
Cr	113	174	134	209	144	125	114	95	128	137.3333	55
Zr	137	145	149	579	359	105	155	92	194	212.7778	210
Rb	18.7	1.9	18.6	3.1	0.5	0.3	0.2	0.2	0.9	4.933333	160
Sr	37.2	7.6	36.5	8.8	9.9	6.7	3.3	10.7	38.1	17.64444	200
Mo	11.52	19.35	13.86	18.86	14.79	20.5	21.2	18.64	26	18.30222	nil
Th	5.73	10.03	24.67	9.77	6.91	2.46	1.37	2.01	3.15	7.344444	6
U	1.02	1.48	2.14	2.57	1.72	1.97	0.65	0.65	3.01	1.69	3.1
Hf	3.8	4.1	4	15.2	9.1	2.7	3.8	2.4	4.9	5.555556	nil
V	23	39	24	36	45	47	10	10	23	28.55556	150
Ni	6.1	5.3	5.5	5.3	5.6	2.3	4	4.3	2.8	4.577778	55
Zn	7	5	8	6	5	4	1	5	11	5.777778	85
Pb	7.4	5.5	5.8	5.8	3.4	1.6	1.3	1.6	4.1	4.055556	20
Cu	4	3.5	3.1	5.3	2.2	22.7	2.7	2.2	4.4	5.566667	50
Ta	0.9	1	1.1	1.4	1.1	0.1	0.2	0.1	0.3	0.688889	nil
As	0.6	0.9	1.4	1	0.6	1.5	0.5	0.6	3.4	1.166667	nil
Cs	0.54	0.27	0.5	0.15	0.05	0.03	0.04	0.03	0.05	0.184444	nil
W	2	1	1	1	1	1	1	1	1	1.111111	nil
Ga	11.8	14.6	12.1	14.8	10.8	3.3	0.9	2	3	8.144444	nil
Nb	5	6.5	6.5	7.5	6.3	1.8	2.2	1.4	3.1	4.477778	1.9
Yb	1.01	0.84	1.36	2.12	1.31	0.44	0.36	0.42	1.02	0.986667	1
Total	627.62	487.77	701.53	991.37	651.78	362.9	331.72	270.35	518.93	549.33	1647

Table 3: Rare earth element data of Agbaja Plateau sandstones

	AA	AC	AE	AF	AL	AQ	AS	AU	AW	MEAN	PAAS
La	32.40	26.80	63.80	35.30	17.30	7.20	6.30	6.70	14.90	23.41	38.20
Ce	46.70	40.10	114.60	68.80	34.30	13.30	11.00	12.80	29.20	41.20	345.00
Pr	4.66	4.14	11.89	7.23	3.62	1.42	1.07	1.20	3.63	4.32	nil
Nd	14.40	14.60	40.80	25.10	13.70	5.80	3.50	5.40	18.50	15.76	128.00
Sm	2.40	1.85	7.00	4.18	2.31	1.23	0.72	1.97	8.83	3.39	16.20
Eu	0.48	0.36	0.76	1.09	0.49	0.22	0.11	0.39	2.40	0.70	1.31
Gd	2.33	2.10	5.22	3.99	2.27	0.94	0.60	1.80	9.49	3.19	6.12
Tb	0.30	0.31	0.56	0.58	0.28	0.13	0.07	0.21	1.15	0.40	nil
Dy	1.70	1.78	3.09	3.41	1.78	0.75	0.50	1.20	5.32	2.17	3.05
Ho	0.33	0.33	0.56	0.75	0.35	0.14	0.10	0.19	0.61	0.37	nil
Er	0.93	0.96	1.79	2.34	0.98	0.45	0.31	0.44	1.27	1.05	1.25
Tm	0.14	0.12	0.20	0.33	0.18	0.07	0.05	0.07	0.17	0.15	nil
Lu	0.13	0.14	0.23	0.33	0.22	0.08	0.06	0.06	0.14	0.15	nil
Y	9.40	10.00	15.40	20.50	10.20	3.60	2.80	3.80	10.80	9.61	nil
∑REE	116.30	103.59	265.90	173.93	87.98	35.33	27.19	36.23	106.41	105.87	539.13
∑LREE	103.37	89.95	244.07	145.69	73.99	30.11	23.30	30.26	86.95	91.97	534.83
∑HREE	12.93	13.64	21.83	28.24	13.99	5.22	3.89	5.97	19.46	13.91	4.30
∑LREE/∑HREE	7.99	6.59	11.18	5.16	5.29	5.77	5.99	5.07	4.47	6.61	124.38

Discussion

Provenance and Paleotectonic setting

Felsic rocks are characterized by high ∑ LREE/∑ HREE ratios and negative Eu anomaly whereas mafic rocks usually show low ∑LREE/∑HREE ratios and no Eu anomalies (Taylor and McLennan, 1985; Bai et al., 2015; Song et al., 2018; Ojo et al., 2021) . The investigated Agbaja Plateau sandstones generally show high ∑ LREE/∑ HREE ratio which indicates felsic origin (table 4) . This conforms with the submission of

Nton and Adamolekun (2016) ; Ojo et al., (2015; 2021) on provenance of sandstones in the southern Bida Basin. The Europium anomaly Eu/Eu* or Eu (anom)) was calculated as:

$Eu/Eu^* = Eu_N / (Sm_N + Gd_N)^{1/2}$ – according to McLennan (1989) .

Liu et al. (2015) stated that Eu/Eu* greater than 1 indicates positive anomaly which is typical of highly feldspathic rock while Eu/Eu* less than 1 connotes negative anomaly which signifies depletion of feldspar. The Eu/Eu* for Agbaja Plateau sandstones are less than 1 which shows that there is depletion of feldspar in the sandstones investigated (Table 4) andthis indicates that the sandstoneshave been subjected to weathering. This is corroborated by dominantly low concentrations of Na_2O, K_2O and CaO. Yu et al. (2022) suggested that Eu (anom) less than 0.85 indicate that the protoliths are mainly granites formed during Late Archean with admixture of Archaean sediments.This suggests that Agbaja Plateau sandstones,with dominantly Eu/Eu* less than 0.85, were sourced from largely granitic provenance.Andersson et al. (2004) proposed Al/Ti ratio ranging from 21 to 70 for felsic protoliths and 8 to 21 for intermediate. High Al/Ti ratio (dominantly above 21) was obtained for the sandstones which supports dominant felsic provenance. The basal sandstones also show high Al/Ti ratio indicating high alumina probably sequel to presence of feldspar and some clay minerals which may have resulted from weathering of feldspar or probably diagenesis suggesting short transportation history. High concentration of Zr and its associated Hf also indicate dominant felsic detritus.McLennan et al. (1993) suggested that Cr/V less than 8 is indicative of felsic provenance while Cr/V greater than 8 indicates mafic provenance. Based on this proxy, Agbaja Plateau sandstones have felsic source with Cr/V less than 8. The high values of Zr/Cr (0.84 to 2.77) also suggest felsic provenance which is applicable to Agbaja Plateau sandstones, as Cr is mainly associated with mafic source and Zr mostly with felsic source (Table 4) . The provenance discrimination plot of Al/Ti vs SiO_2 after Le Bas et al. (1986) (Fig. 8) indicates felsic source. TiO_2 vs Zr provenance discrimination plot after Hayashi et al. (1997) shows origin of felsic igneous rock (Fig. 9a) . Palaeotectonic bivariate plot of log (Na/K) vs Si after Roser and Korsch (1986) shows that the sandstones were deposited in passive margin tectonic setting (Fig. 9b).

Maturity, Palaeoweathering and Palaeoclimate

The plot of CIA vs SiO_2 (Fig. 10a) shows that the sandstones are mainly kaolinitic which indicates their intense weathering history. The palaeoclimatic plot of Si vs (Al+Na+K) , (Fig. 10b) shows variation in humidity in the history of Bida Basin with less humidity in the early history (Campanian) and increasing humidity later in Maastrichtian. The plot of PIA vs CIA after Abedini and Calagari (2017) also shows extreme silicate weathering (Fig.11a) . The high SiO_2 (varies from 92.06% to 97.49%) and lower alumina (0.73% to 2.02%) of the upper sandstones suggest higher mineralogical maturity compared to the sandstones at the lower part of the section (SiO_2 varies from 73.3% to 82.69% while alumina varies from 9.4% to 15.75%) . Generally, the palaeoweathering indices (PIA, CIA, CIW in Fig. 11b) are high, therefore, corroborating high intensity weathering. The seemingly low palaeoweathering indices, despite being unfeldspathic, upsection is due to very low Al_2O_3 and generally low Na_2O, K_2O and CaO almost across the section. The 15.75% peak alumina in bed F may be due to clayey

Table 4: Geochemical proxies for Agbaja Plateau sandstones

	AA	AC	AE	AF	AL	AQ	AS	AU	AW
Zr/Ti	507.41	439.39	438.24	1346.51	997.22	1166.67	1409.09	1150.00	1212.50
Na/Al	0.00	0.00	0.00	0.00	0.00	0.01	0.01	0.00	0.01
Zr/Cr	1.21	0.83	1.11	2.77	2.49	0.84	1.36	0.97	1.52
Al+Na+K	12.81	12.66	12.06	15.92	9.43	1.45	0.77	2.06	1.60
Al/Ti	44.52	38.21	32.85	36.63	26.11	15.67	6.64	25.25	9.50
K/Na	12.17	4.00	16.80	4.67	2.00	3.00	3.00	3.00	7.00
Sr/Ba	0.16	0.19	0.15	0.15	0.42	0.54	0.41	0.53	0.60
P/Ti	0.04	0.03	0.06	0.02	0.06	0.56	0.09	0.13	0.63
V/Cr	0.70	1.18	0.73	1.09	1.36	1.42	0.30	0.30	0.70
Cr/V	1.14	0.85	1.37	0.92	0.74	0.70	3.33	3.33	1.14
U/Th	0.03	0.04	0.06	0.07	0.05	0.05	0.02	0.02	0.08
Ba/Al	19.16	3.24	22.24	3.73	2.50	8.87	10.96	9.95	41.91

Table 4 continued: Geochemical proxies of Agbaja Plateau sandstones continued

	AA	AC	AE	AF	AL	AQ	AS	AU	AW
V/(V+Ni)	0.79	0.88	0.81	0.87	0.89	0.95	0.71	0.70	0.89
Zr/Rb	7.33	76.32	8.01	186.77	718.00	350.00	775.00	460.00	215.56
Fe/Mn	318.00	390.00	260.00	161.00	267.00	414.00	158.00	151.00	631.00
Cu/Zn	0.57	0.70	0.39	0.88	0.44	5.68	2.70	0.44	0.40
CIW	99.09	99.76	99.29	99.56	96.31	98.60	97.33	99.02	98.70
PIA	99.04	99.76	99.23	99.55	96.30	98.57	97.22	99.00	98.64
ICV	0.37	0.34	0.35	0.25	0.36	3.05	2.41	0.82	4.33
CIA	93.47	99.45	92.39	98.68	96.11	96.58	93.59	97.58	94.41
Th/U	37.25	25.68	17.76	14.79	22.09	19.29	58.46	58.46	12.62
Rb/Sr	0.50	0.25	0.51	0.35	0.05	0.04	0.06	0.02	0.02
Sr/Cu	9.30	2.17	11.77	1.66	4.50	0.30	1.22	4.86	8.66
Ti/Al	0.02	0.03	0.03	0.03	0.04	0.06	0.15	0.04	0.11
(Cu+Mo)/Zn	2.22	4.57	2.12	4.03	3.40	10.80	23.90	4.17	2.76
Ni/Al	0.51	0.42	0.49	0.34	0.60	1.63	5.48	2.13	1.84
Cu/Al	0.33	0.28	0.28	0.34	0.23	16.10	3.70	1.09	2.89
Zn/Al	0.58	0.40	0.72	0.38	0.53	2.84	1.37	2.48	7.24
La/V	1.41	0.69	2.66	0.98	0.38	0.15	0.63	0.67	0.65
Si/Al	6.38	5.81	7.23	4.77	8.80	67.78	133.55	47.90	60.57
U-(Th/3)	-0.89	-1.86	-6.08	-0.69	-0.58	1.15	0.19	-0.02	1.96
Ti/Ca	5.40	16.50	11.33	10.75	1.03	9.00	11.00	8.00	16.00
Eu(anom)	0.50	0.41	0.51	0.87	0.52	0.35	0.22	0.46	1.27
(La/Yb)n	0.84	0.84	1.23	0.44	0.35	0.43	0.46	0.42	0.38
(La/Sm)n	5.73	6.14	3.87	3.58	3.18	2.48	3.71	1.44	0.72
(Gd/Yb)n	0.38	0.41	0.63	0.31	0.28	0.35	0.27	0.70	1.52
(Sm/Nd)n	1.32	1.00	1.36	1.32	1.33	1.68	1.63	2.88	3.77
Th/U	5.62	6.78	11.53	3.80	4.02	1.25	2.11	3.09	1.05
V/Ni	3.77	7.36	4.36	6.79	8.04	20.43	2.50	2.33	8.21

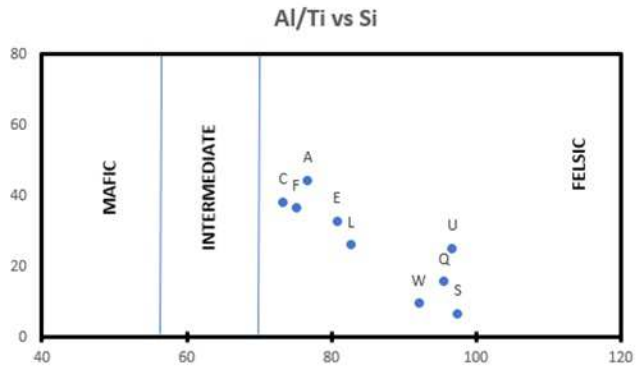


Fig. 8: Provenance discriminatory plot of Al/Ti vs Si (after Le Ba et al., 1986) showing felsic provenance for the investigated Agbaja Plateau sandstones.

content arising from weathering of feldspar. The low Si/Al obtained from the basal sandstones may also be attributed to weathered feldspar or probably short period of transportation which allows preservation of feldspar and probably other aluminosilicate minerals. High Si/Al also indicate higher mineralogical maturity for the sandstones upsection compared to the sandstones at the lower part of the section.

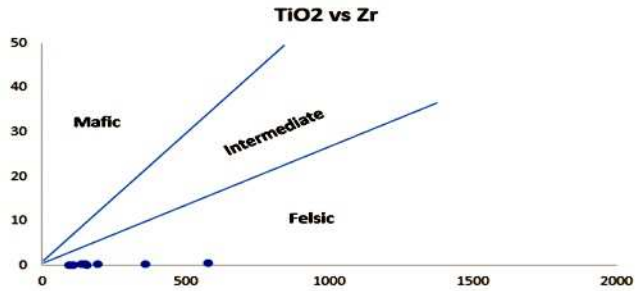


Fig. 9a: Plot of Ti vs Zr (after Hayashi et al., 1997) showing felsic source for the sandstones

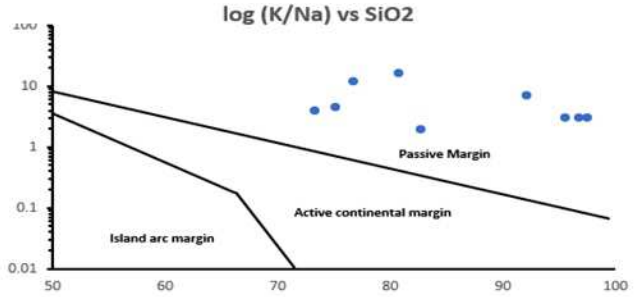


Fig. 9b: Paleotectonic plot of log (K/Na) vs Si (after Roser and Korsch, 1986) indicates the sandstones were deposited in passive margin setting

Rb seems more stable than Sr in the course of weathering. Hence, Rb is easier to retain than Sr (Chen et al. 2000) . Sr is easily weathered in humid climate. Hence, increase in the Rb/Sr ratio may be typical of humid setting. In dry climate, there is less rainfall and low weathering, Sr retention may be high due to reduced or aborted weathering. This can lead to a decrease in Rb/Sr value**.** Hence, low Rb/Sr value indicate dry palaeoclimate while high Rb/Sr indicate wetness. The profile plots of Th/U and Rb/Sr (Fig.11b) were used to constrain the palaeoweathering interpretation. The Th/U values are generally low showing humid condition as evident in the slight variation ranging from semi-humid to humid along the vertical section shows probably a mild palaeoclimatic variation in the sedimentation history of the Bida Basin. This may be connected with global temperature rise in the Cretaceous which might have favoured weathering at various stages. Rb/Sr was keenly studied by Chang et al. (2013) for palaeoenvironmental deduction. They suggested high Rb/Sr for low weathering rates while low Rb/Sr mean high weathering rate. They argued that due to weathering, Sr gets leached more during periods of strong weathering than Rb. The Rb/Sr is generally low showing high intensity of weathering and dominantly humid and oxic condition of deposition.

When Sr/Cu is greater than 5, it means dry and hot climate, 1.3 to 5.0 means warm and humid (Wang et al., 1997; Liu and Zhou, 2007) . The warm, humid climatic condition promotes more weathering which is the case for upper sandstones unlike the basal sandstons which plot mainly at hot and dry palaeoclimatic condition. The profile plot also shows variation in palaeotemperature in theearly history of the basin. The boundary between the immature sandstones and the more mature upper sandstones bears a low temperature regime at Campano-Maastrichtian boundary. The plot also reaveals increasing palaeotemperature in the Maastrichtian which is consistent with the submission ofBodin et al. (2015).

Paleo-Oxygenation

Elements such as Fe, U, Co, Cr, V, Ni are some of the redox sensitive elements (Omietimi et al., 2022) as most of them are immobile after deposition and burial. V/Cr greater than 4.25 is an indication of anoxic depositional setting, 2.0 to 4.25 is dysoxic while less than 2 is oxic (Jones and Manning, 1994) . U/Th greater than 1.25 is anoxic, 0.75-1.25 is dysoxic, less than 0.75 is oxic (Jones and Manning, 1994) . The U/Th is generally less than 0.75 which signify oxic condition according to

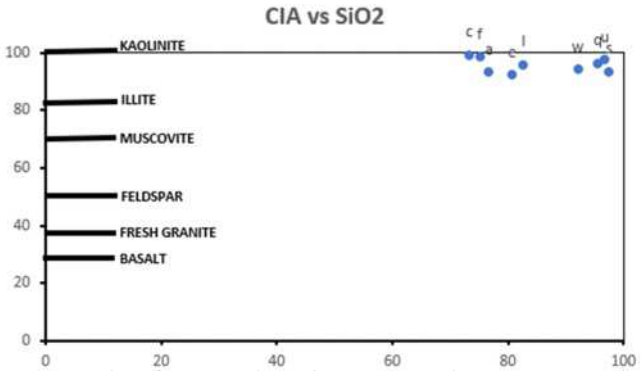


Fig. 10a: Plot of CIA vs SiO2 after Suttner and Dutta (1986) . The sandstones plot in kaolinitic field suggesting high maturity probably due to intense weathering

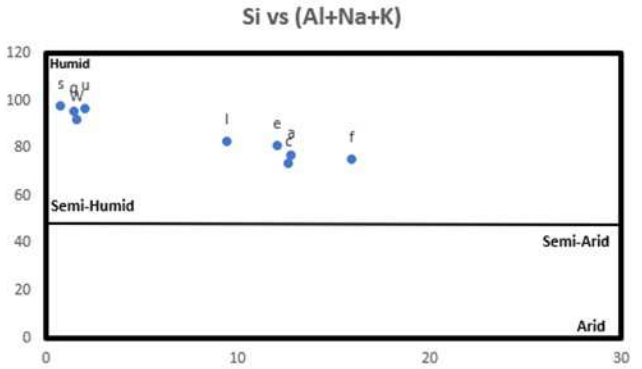


Fig. 10b: Plot of Si vs (Al+Na+K) after Suttner and Dutta (1986) . The basal sandstones plot in less humid field while others plot in more humid field showing humidity variation in the history of Bida Basin.

Jones and Manning (1994) . Similarly, Cu/Zn is used for paleoredox indicator. The ratio is generally low which signify oxic condition. The high values mean reducing condition (Fig. 12) . Hallberg and Xannbepr (1976) proposed (Cu+Mo) /Zn greater than 2 as indicative of oxic and vice versa. Wignall and Myers (1988) provide reference via U-Th/3 and used it to estimate paleoredox condition. In this present study, the V/Cr is generally below 2 which signify oxic condition (see Table 4 and Fig. 12) . U/Th is also less than 0.75 indicating oxic condition except the spike at the upper part of the section. Cu/Zn is also generally low suggesting oxic depositional condition. The low values of U- (Th/3) and (Cu+Mo) /Zn greater than 2 indicate dominant oxic condition. U/Th profile shows spike towards the transition zone and the upper part of the section supporting less oxic condition at the transition zone and the upper section. Ojo et al. (2020) reported occurrence of shale below the ironstone cap at Agbaja Plateau. This may be why U/Th spike is suggesting probable brief anoxic condition at the upper part of the section. The restricted spikes of other proxies in the upper part of the section suggest changing paleo-oxygenation condition to probably less oxic.

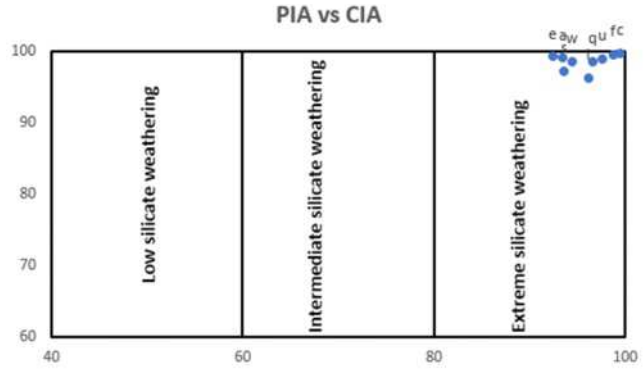


Fig. 11a: Plot of PIA vs CIA (after Abedini and Calagari, 2017) showing the sandstones have undergine intense weathering

Paleohydrodynamics and Paleodepth

Zr/Rb has been used to predict paleo-water depth and paleohydrodynamics (Pehlivanli, 2019) . Zr/Rb less than 0.92 implies weak paleohydrodynamic regime, 1.25-4.76 means immediate, greater than 4.76 suggest high hydrodynamic regime (Teng, 2004) . Fe/Mn (Wang et al., 2020) is also good for paleodepth indicator. The high ratio indicates shallow water depth.From Fe/Mn profile (Fig. 14) , the paleowater depth is deeper upsection compared to the lower part of the section probably due to marine incursion in the Maastrichtian.

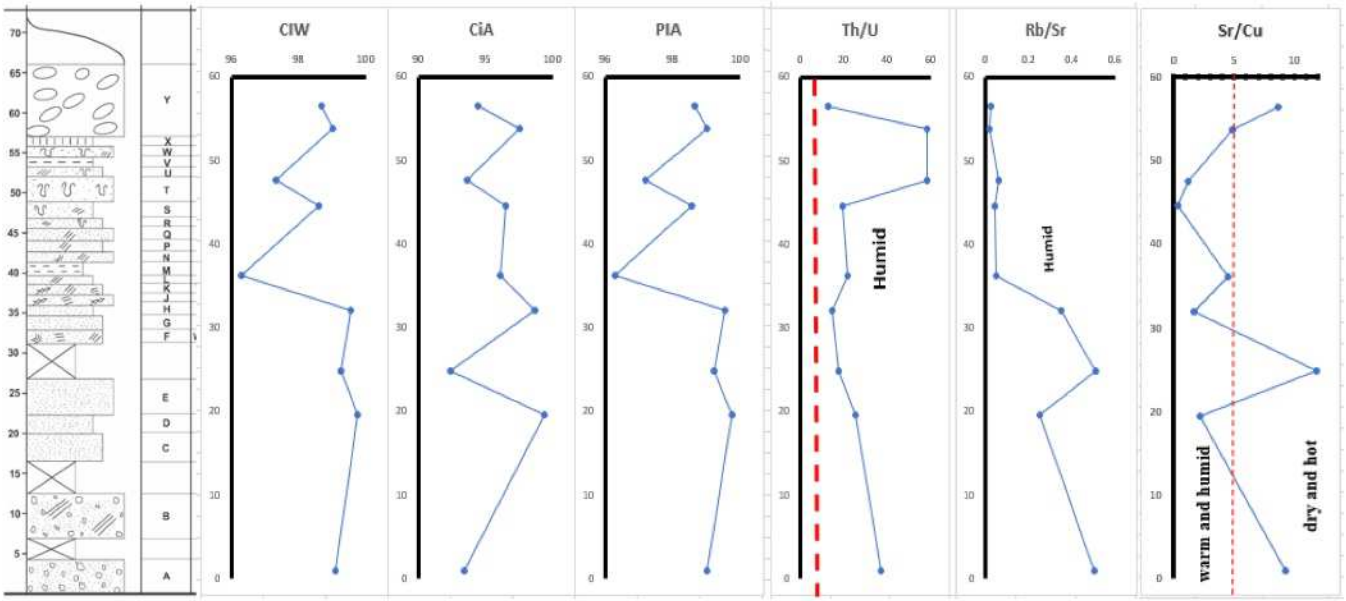


Fig. 11b: Paleoweathering profile plot (CIA, PIA, CIW) showing intense weathering (with values greater than 90%) and paleoclimatic (Th/U, Rb/Sr, Sr/Cu) profile plot showing dry and less humid condition in the early history of the basin and domiant warm to humid condition in the latter stage

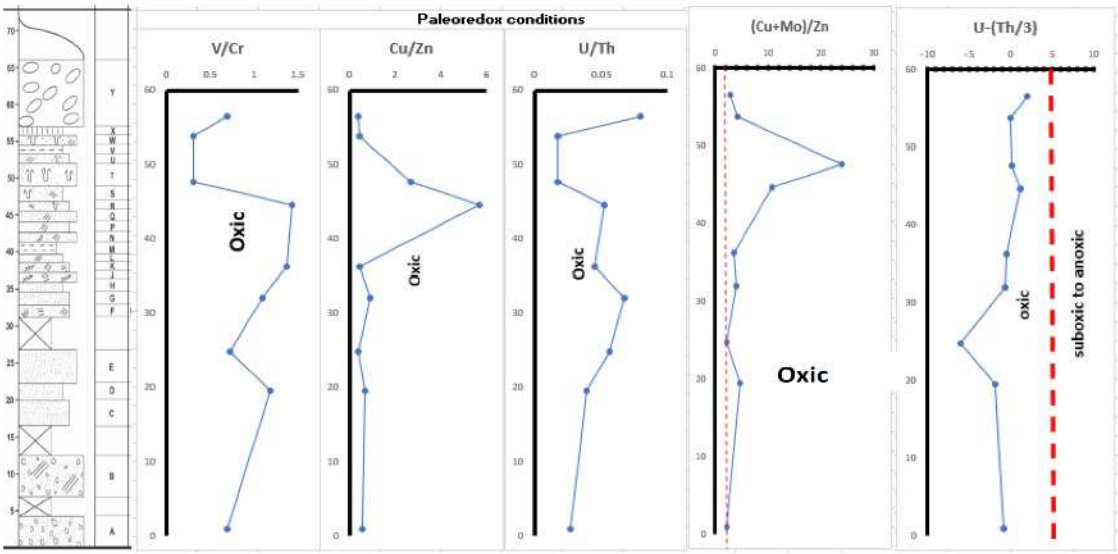


Fig. 12: Paleo-oxygenation profile plot showing more oxic aondition in the Campanian and brief less oxic phase in the Maastrichtian

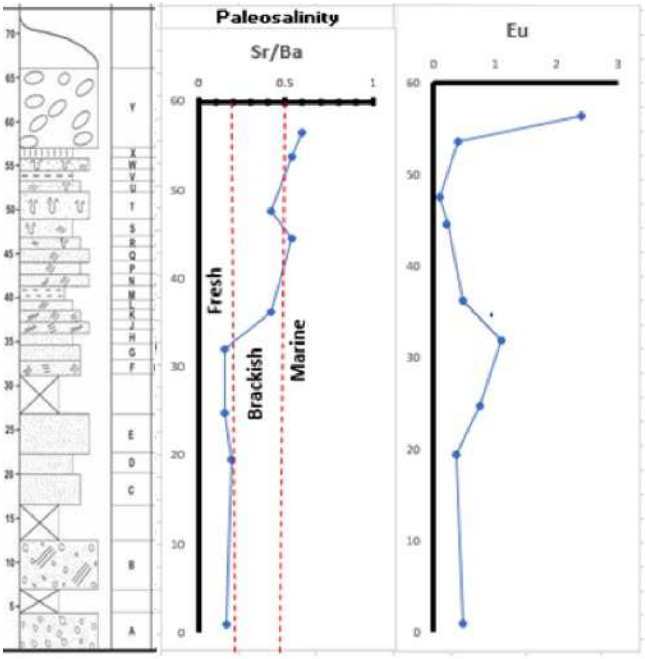


Fig. 13: Paleosalinity profile plots showing marine incursion at the upper part of the section in the Maastrichtian

This is supported by stronger paleohydrodynamics (Zr/Rb profile plot – Fig. 14) in the Maastrichtian than in the Campanian. The marine incursion increases the paleohydroenergy of the depositing medium. This supports the documented shale at Agbaja Plateau by Ojo et al. (2020).

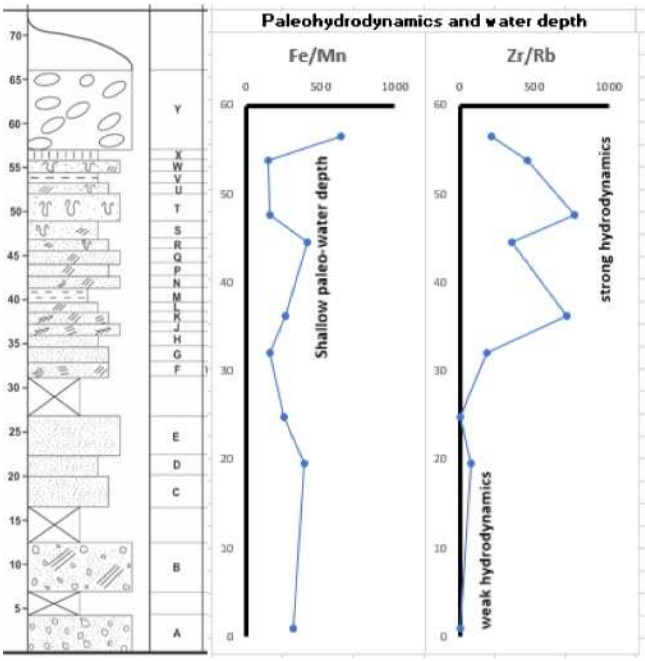


Fig. 14: Profile plots for paleohydrodynamics and paleowater depth showing variation in paleowater depth with dominant shallow water depth ad stronger hydroeneergy in the Maastrichtian probabaly due to marine incursion

Paleohydrodynamics and Paleodepth

Sediment Deposition Rate, Terrestrial Detritus Influx and Glaciation

Wang et al. (1989) postulated that (La/Yb) n, n-normalized to PAAS of Taylor and McLennan, (1985) , is a proven proxy to infer sediment deposition rate. The low values of (La/Yb) n suggest low deposition rate and high values suggest high depositional rate.High Ti/Al may also suggest low deposition rate and vice versa. Al and Ti are higher in regressive system showing likely high detritus influx than in a transgressive system (Song et al., 2018) . This means high Al and Ti indicate high derital influx and probably high sedimentation rate.The concentration of aluminum in sediments may indicate supply of terrigenous clasts because Al is sourced mostly from clay minerals (Lezin et al., 2013; Algeo and Maynard, 2004) . At times the Al in sediments may be authigenic, but Ti is not (Wei et al., 2003) . The high sum of REEs may amount to high terrigenous deposition (Venancio et al., 2018) . This can be attributed to very low sea-level (Waelbroeck et al., 2002) .This agrees with low temperature and relatively low sea level at Campanian-Maastrichtian boundary proposed (Fairhead and Binks, 1991; Binks and Fairhead, 1992; Skelton et al., 2003; Bodin et al., 2015; Edegbai et al., 2019) . Hence, the Campanian-Maastrichtian may be a period of glaciation that led to high regression. The glacial period can also be recorded at low (near zero) Ti/Ca profile according to (Govin et al, 2012; Nace et al., 2014) (Fig.15) . This is corroborated by palaeotemperature inference from Sr/Cu (Fig.11b) . In Figure 15, the high values of (La/Yb) n, (La/Sm) n at the lower part of the section suggests high deposition rate and lower deposition rate for sandstones upsection.

Zr/Ti spikes mean increased detritus input which may also signify climatic change. As Zr is strictly restricted to zircon which is mostly associated with acid igneous rocks and some metamorphic. V/Ni canbe used to probe the origin and the depositional environment of the organic matter. V/Ni values less than 1.9, 1.9 to 3 and greater than 3 indicate terrestrial organic matter, organic matter of mixed marine and terrestrial source and marine organic matter respectively (Akinlua et al., 2016; Zhao et al., 2017) . The V/Ni are dominantly greater than 3 (Fig. 16) showing dominance of marine organic matter, even in the Campanian sandstones, thereby suggesting brief marine incursion in the Campanian as well. The Maastrichtian upper sandstones show higher V/Ni and support more marine incursion (probably tidal setting as reported by Ojo and Akande,

2009) rather than continental detritus at the time the upper sandstones were deposited.

At Agbaja Plateau (Fig. 15) , Al and Ti profiles show higher detrital at the lower part of the section than upsection. This supports more marine influence upsection as inferred by Sr/Ba. The reduced detritus upsection also supports inferred less oxic condition upsection. Zr/Ti also show the basal sandstones are more of regressive deposits while the upper sandstones are transgressive (sediments trasported into the basin from afar) . The Zr/Ti profile support intrabasinal sediment source for basal sandstone and extrabasinal source for upper sandstone. This supports marine incursion in the upper sandstone. It also shows that the transgression changed the sedimentary facies in the Bida Basin. This is supported by more pervasive tidal-related sedimentary structures were seen at Agbaja Plateau (earlier reported by Ojo and Akande, 2009) . The high Zr/Ti upsection indicates more maturity. This concurs with paleosalinity interpretation.The regressive glacial peak period is suspected in low Ti/Ca (as used in siliciclastic system by Govin, et al, 2012; Nace et al., 2014) where the profile plot tends to zero thereby suggesting near zero deposition and probably a thermal low – period of glaciation. EREE (supported by La/Yb, La/Sm – all normalized to PAAS of Taylor and McLennan, 1985).

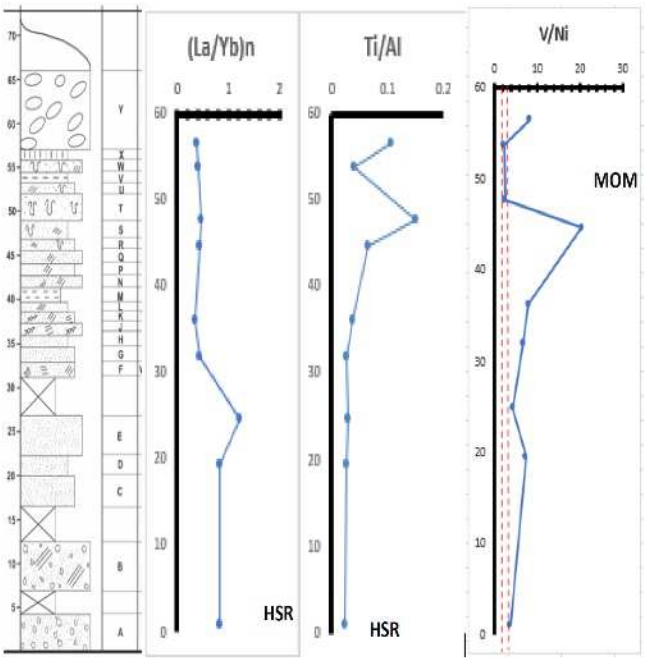


Fig. 15: Profile plots showing sedimentation rate was faster upsection and slower for the lower part of the section. HSR – High Sedimentation Rate. MOM – Marine Organic Matter

Paleoproductivity

Paleoproductivity depends on organic matter supply by surface water and presence or absence of microbes that can degrade the organic matter (Cheng et al., 2021) . Paleoproductivity is the basis for the enrichment of the organic matter in marine sediments. Elements such as P, Ba, Si, Cu, and Ni are essential trace elements for biological life activities. The availability of these elements in sediments can signify paleoproductivity (Tribovillard et al., 2006; Algeo et al., 2011; Schoepfer et al., 2015) . Ba/Al and P/Ti can reveal nutritional conditions and paleoproductivity. Organic matter availability is not unconnected to P and Ba availability (Tribovillard et al., 2006) . P/Ti less than 0.34 means low productivity, 0.34 to 0.79 is intermediate while values greater than 0.79 means high paleoproductivity (Li et al., 2020) .

Furthermore, Ni/Al, Zn/Al and Cu/Al can all be used as proxies for paleoproductivity (Algeo and Maynard, 2004) . The low values of these proxies point to low paleoproductivity while the high values will signal high paleoproductivity. The three proxies show generally low values indicating dominantly low paleoproductivity.

In Figure 17, P/Ti, Zn/Al and Ba/Al are generally low but increased at the upper part of the section, suggesting high paleoproductivity and organic richness. Also, Ni/Al, Cu/Al and Na/Al are generally low for sandstones at the lower part of the section but spiked mainly at the upper part of Agbaja Plateau which may suggest surge in paleoproductivity which might have resulted from inferred marine incursion and subsequent less oxic setting. The dominantly low paleoproductivity support dominant oxic and humid setting across the section.

Diagenesis, Maturity and Sediment Recycling

Trueman and Tuross (2002) suggestedthat enrichment of Chromium to Vanadium may signify a level of diagenesis. They recommended V/Cr less than 2 (Fig.18) to mean a certain degree of diagenesis while V/Cr greater than 2 may indicate low diagenesis. The profile plot shows that the sandstones have been subjected to diagenesis. High ratios ofZr/Ti can be used to interpret progressive maturity (Zhang et al., 2004) . Armstrong-Altrin et al. (2014) recommended K/Na ratio greater than 1 for high chemical maturity and sediment recycling. The spike in K/Na at the transition zone might have resulted from the presence of K-rich

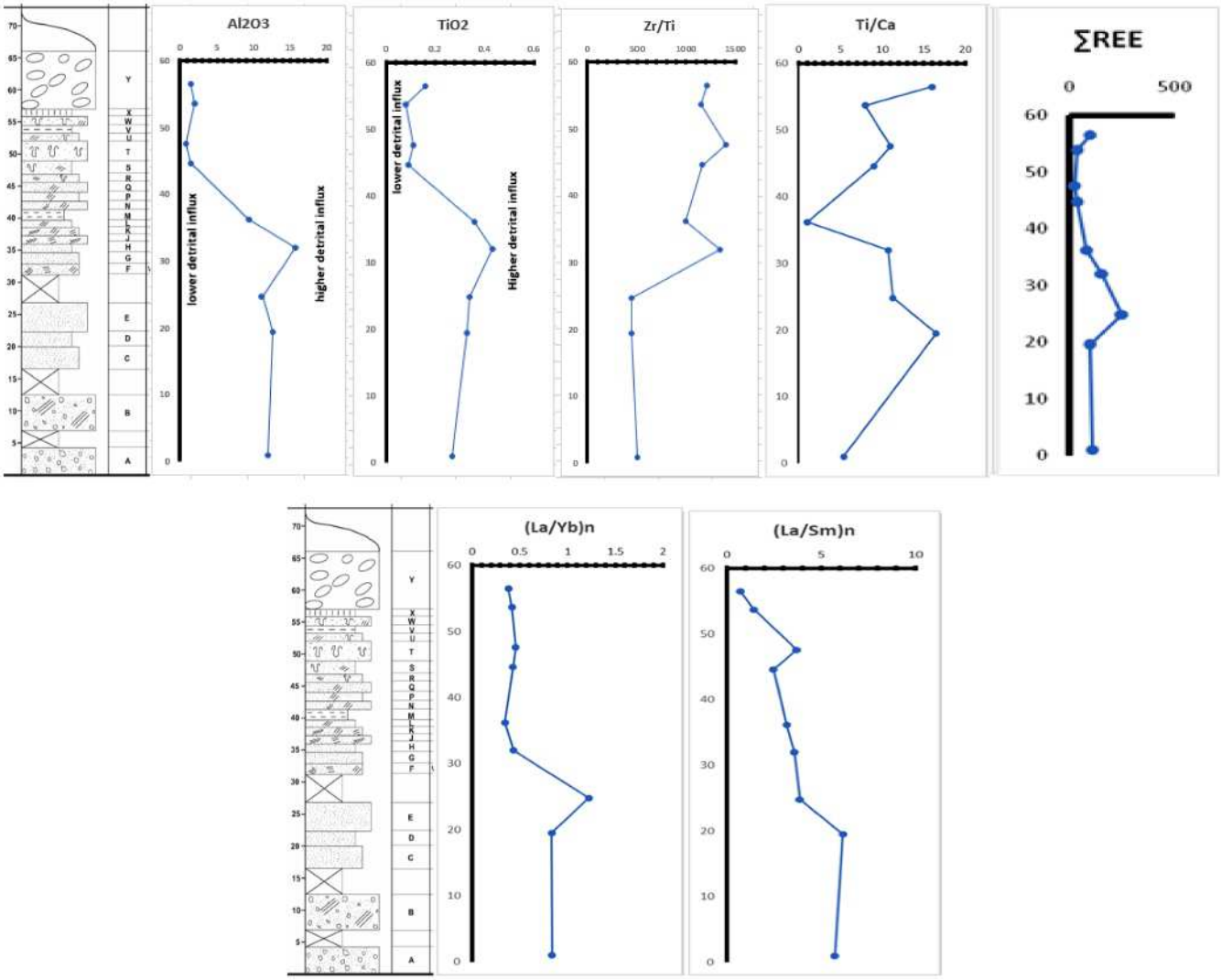


Fig. 16: Profile plots showing higher terrestrial influx at the lower part of the section and lower influx at the upper part of the section.

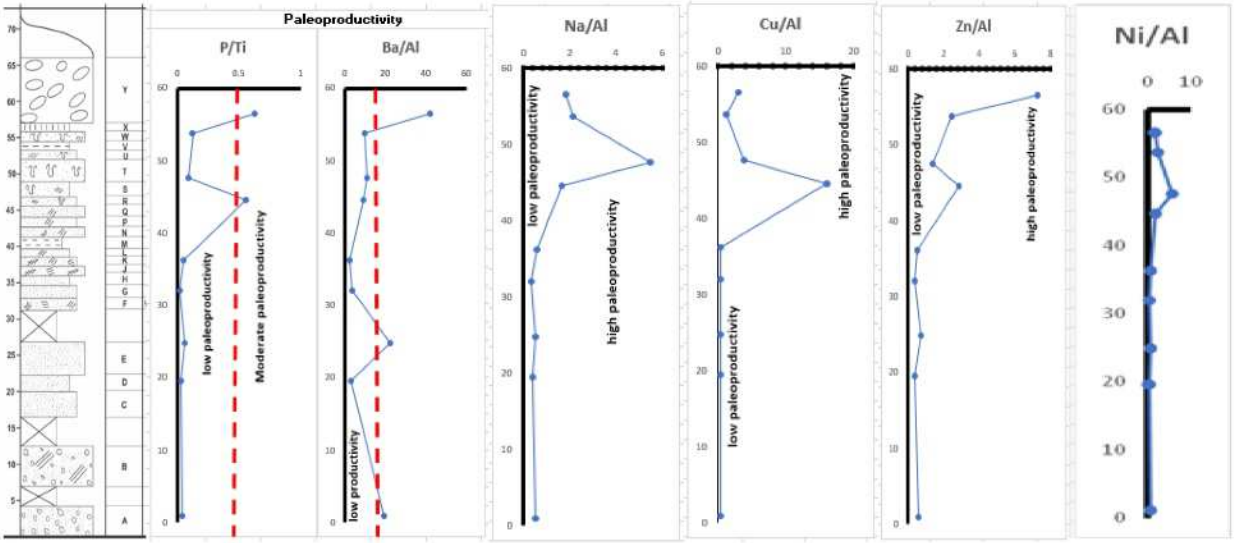


Fig. 17: Paleoproductivity profile plots showing spike in paleoproductivity at the upper part of the section which corroborates inferred less oxic condition and high sedimentation rate which might have aided preservation of organic matter

clay minerals sequel to weathering and diagenesis. Roser et al. (1996) suggested Si/Al less than 3 means basic igneous, 3 to 5 means acid igneous rocks while greater than 5 in clastic sediment suggests high sediment maturity.

High sediment recycling may also be inferred from elevated values of (Gd/Yb) n in sandstones as demonstrated by (McLennan, 1989; Kandemir et al., 2022) . This corroborates sediment recycling interpretation from K/Na profile plot. Also, high sum of REEs was suggested as high sediment recycling and possible control by different amount of accessory minerals (Zou et al., 2016) . In all, the transition zone seems to be the period of highest sediment recycling and this may also indicate that this is a zone of intense weathering. Other climatic inputs such as moist sediment deposition, high precipitation and erosion may also be responsible for increased REEs (Sousa et al., 2022) . Less ∑ REE may imply high sea level and probably high temperature. Increase in the sea level reduces continental materials. High Fe_2O_3 may also signify high continental detritus input (see table 1) V/Cr indicate values indicate that the sandstones from Agbaja Plateau have been subjected to a degree of diagenesis (Fig. 18) . Notably the uppermost sandstones have undergone more diagenesis than the lower sandstonesand this may be due to longer transportation and marine reworking. Alumina, K and Al reduces upsection which is in line with increasing diagenesis. The low ∑REE also support marine incursion and higher temperature later in the Maastrichtian than Campanian. High Si/Al upsection support high chemical maturity and it further supported by high Zr/Ti and low La/V (Fig. 18).

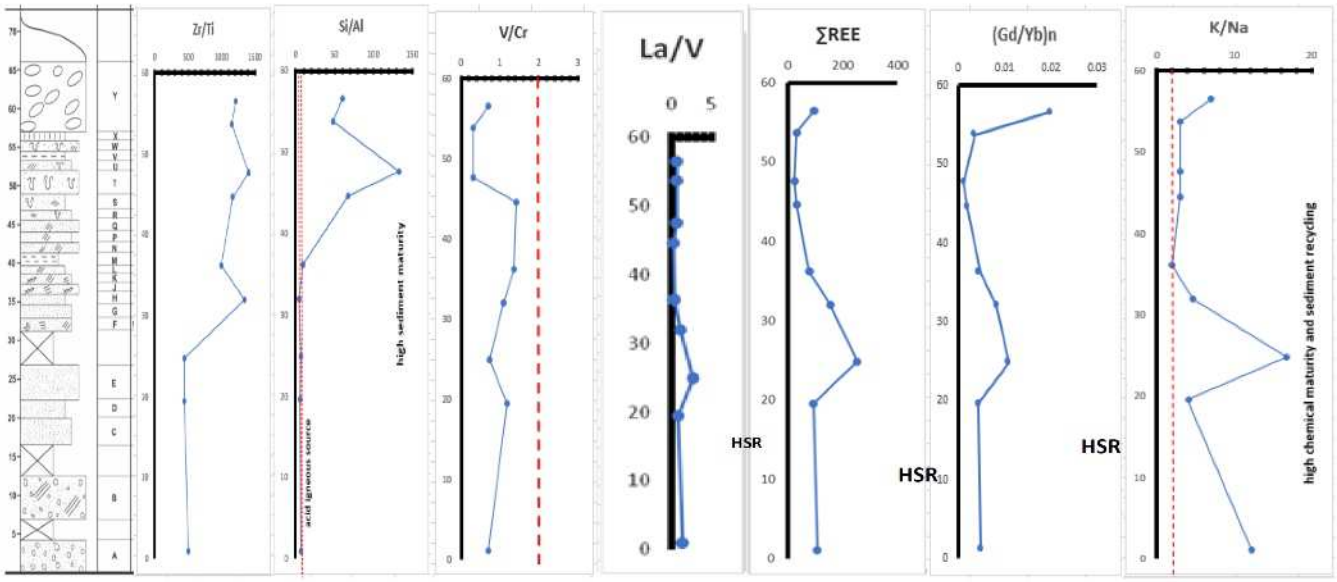


Fig. 18: Profile plots of diagenesis and sediment recycling shwing that the sandstones have undergone a degree of diagenesis and sediment recycling was more pervasive in the lower part of the section compared to the upper part. HSR – High Sediment Recycling

Conclusions

Agbaja Plateau sandstones were deposited in dominantly oxic condition with brief anoxic phase recorded at the upper part of the section during the Maastrichtian. The less oxic phase may be responsible for spike in organic matter richness in the Late Maastrichtian. The basal sandstones are characterised by low paleoproductivity while the sandstones at the upper part of the section showed spike in paleoproductivity. The marine organic matter composition of the sandstones was diluted by high terrigenous input and high sediment recycling. The boundary between the basal sandstone and upper sandstone probably represents a low-temperature regime.

The sandstones are of felsic origin and were deposited in passive margin setting. The sandstones at the upper partof the section are more weathered and mature than the basal sandstones which suggests relatively low humidity in the Campanian and high humidity in the Maastrichtian and therefore indicate changing paleoclimate, paleotemperature and paleosalinity over time in the late Cretaceous.

The sandstones at the upper part of Agbaja Plateau section experienced more marine incursion in the Maastrichtian, probably via connected Tethys and south Atlantic Ocean. This also reflects a stronger hydrodynamic regime in the Maastrichtian time.

Acknowledgement

This research benefitted from Tetfund NRF 2020 Grant and Tetfund AST and D. The management of the Federal University also provided valuable support for the research. The anonymous reviewers are gratefully acknowledged for their useful suggestions.

References

Abedini, A. and Calagari, A.A. (2017) . Geochemistry of claystones of the Ruteh Formation, NW Iran: Implications for provenance, source-area weathering, and paleo-redox conditions. N. Jb. Miner. Abh. (Journal of Mineralogy and Geochemistry) , 194 (2) , pp. 107–123

Adegoke, J.A. and Layade, G.O. (2014) . Application of thin sheet model for the analysis and interpretation of aeromagnetic data. Research Journal of Physics, 8 (1) , p. 28-37, DOI: 10.3923/rjp.2014.28.37

Adeleye, D.R. and Dessauvagie, T.F.J. (1972) . Stratigraphy of the Niger Embayment near Bida, Nigeria. In: T. F.J. Dessauvagie and A. J. Whiteman (eds) , African Geology, University of Ibadan Press, pp.181-186

Agyingi, C.M. (1991) . Geology of upper Cretaceous rocks in the eastern Bida Basin, Central Nigeria: Unpublished Ph.D. Thesis, University of Ibadan, Nigeria, pp. 501.

Agyingi, C.M. (1993) . Palynological evidence for a late Cretaceous age for Patti Formation, Eastern Bida Basin, Nigeria. Journal of African Earth Sciences, 17, pp. 513–523.

Akande, O.S., Ojo, O.J., Erdtmann, B.D. and Hetenyi, B.M. (2005) . Paleoenvironments, organic petrology and Rock-Eval studies on source rock facies of the Lower Maastrichtian Patti Formation, southern Bida Basin, Nigeria. Journal of African Earth Sciences, 41, pp. 394–406

Akinlua, A., Olise, F.S., Akomolafe, A.O. and McCrindle, R.I. (2016) . Rare earth element geochemistry of petroleum source rocks from northwestern Niger Delta. Marine and Petroleum Geology, pp. 77.

Algeo, T.J. and Maynard, J.B. (2004) . Trace-element behavior and redox facies in core shales of Upper Pennsylvanian Kansas-type cyclothems. Chemical Geology, 206, pp. 289 – 318

Algeo, T.J., Chen, Z.Q., Fraiser, M.L., and Twitchett, R.J. (2011) . Terrestrial–marine teleconnections in the collapse and rebuilding of Early Triassic marine ecosystems. Palaeogeography Palaeoclimatology Palaeoecology, 308 (1) , pp. 1– 11

Andersson, P.O.D., Worden, R.H., Hodgson, D.M. and Flint, S. (2004) . Provenance evolution and chemostratigraphy of a Palaeozoic submarine fan-complex: Tanqua Karoo Basin, South Africa. Marine and Petroleum Geology, 21, pp. 555 – 577.

Armstrong-Altrin, J.S., Nagarajan, R., Lee, Y.I., and Córdoba-Saldaña, L.P. (2014) . Geochemistry of sands along the san Nicolás and san Carlos beaches, Gulf of California, Mexico: implication for provenance. Turkish Journal of Earth Science., 23, pp. 533–558.

Bai, Y.Y., Liu, Z.J., Sun, P.C. (2015) . Rare earth and major element geochemistry of Eocene fine-grained sediments in oil shale- and coal-bearing layers of the Meihe Basin, Northeast China. Journal of Asian Earth Sciences, 97, pp. 89–101

Binks, R.M. and Fairhead, J.D. (1992) . A plate tectonic setting for Mesozoic rifts of West and Central Africa. In: In: Ziegler, P.A. (Ed.) , Geodynamics of Rifting, Volume II. Case History Studies on Rifts: North and South America and Africa.Tectonophysics, 213, pp. 141–151.

Bodin, S., Meissner, P., Janssen, N.M., Steuber, T.andMutterlose, J. (2015) . Large igneous provinces and Organic carbon burial: controls on global temperature and continental weathering during the Early Cretaceous. Global Planet. Change, 133, pp. 238–253.

Braide, S.P. (1992) . Geological development, origin and energy mineral resources potential of the Lokoja Formation in the southern Bida Basin. Journal of Mining and Geology, 28, pp. 33-44.

Calvert, S.E., Bustin, R.M., Pedersen, T.F. (1992) . Lack of evidence for enhanced preservation of sedimentary organic matter in the oxygen minimum of the Gulf of California. Geology, 20 (8) , pp. 757–760.

Chang, H., An, Z., Wu, F., Jin, Z., Liu, W. and Song, Y. (2013) . A Rb/Sr record of the weathering response to environmental changes in westerly winds across the Tarim Basin in the late Miocene to the early Pleistocene. Palaeogeography, Palaeoclimatology, Palaeoecology, 386, pp. 364–373

Chen, J., Wang, Y.J., Yang, C., Liu, L.W., Ji, J.F. and Lu, H.Y. (2000) . Rb and Sr geochemical characterization of the Chinese loess stratigraphy and its implications for palaeomonsoon climate. Acta Geologica Sinica., 74 (2) , pp. 279–288

Chen, Q., Li, Z., Dong, S., Yu, Q., Zhang, C. and Yu, X. (2021) . Applicability of chemical weathering indices of eolian sands from the deserts in northern China. Catena, 198, pp. 1 – 11

Cheng, Y., Jian, L., Tang, G. and Zhang, C.Y. (2021) . Trace element anomaly characteristics and metallogenic significance of the lower Cambrian Qiongzhusi Formation from Huize area, eastern Yunnan province. Nonferrous Metals Science and Engineering, 10 (12) , pp. 90–98

Convers, L.C. (2020) . Paleoenvironment Reconstruction of the Eocene Southeastern Tethys Using Geochemistry of Sedimentary Rocks. Theses, Dissertations and Culminating Projects, pp. 1-46

Edegbai, A.J., Schwarka, L. and Oboh-Ikuenobe, F. E. (2019) . A review of the latest Cenomanian to Maastrichtian geological evolution of Nigeria and its stratigraphic and paleogeographic implications. Journal of African Earth Sciences, 150, pp. 823 – 837

Fairhead, J.D. and Binks, R.M. (1991) . Differential opening of the central and south Atlantic oceans and the opening of the West African, Rift System. Tectonophysics, 187, pp. 191–203.

Frimmel, A., Oschmann, W., Schwark, L. (2004) . Chemostratigraphy of the Posidonia Black Shale, SW Germany: I. Influence of sea-level variation on organic facies evolution. Chemical Geology, 206 (3–4) , pp. 199–230

Govin, A., Holzwarth, U., Heslop, D., Ford, K. L., Zabel, M. and Mulitza, S., (2012) . Distribution of Major Elements in Atlantic Surface Sediments: Imprint of Terrigenous Input and Continental Weathering. Geochemistry Geophysics. Geosystem, 13 (1) , pp. 1–23

Hallberg, R.O. (1976) . A Geochemical Method for Investigation of Paleoredox Conditions in Sediments. Ambio Special Report 4. pp. 139-147

Hayashi, K., Fujisawa, H., Holland, H., and Ohmoto, H. (1997) . Geochemistry of 1.9 Ga sedimentary rocks from northeastern Labrador, Canada. Geochimica et Cosmochimica Acta, 61 (19) , pp. 4115–4137.

Idowu, J.O. and Enu, E.I. (1992) . Petroleum geochemistry of some late Cretaceous shales from the Lokoja sandstone of Middle Niger basin, Nigeria. Journal of African Earth Sciences, 14 (3) , pp. 443–455.

Jan du Chene, R.E., Adegoke, O.S., Adeniran, S.A. and Petters, S.W. (1978) . Palynology and Foraminifera of the Lokoja Sandstone (Maastrichtian) , Bida Basin, Nigeria. Revista Epanola de Micropaleontologia,10, pp. 379 – 393

Jones, H.A. (1958) . The oolitic ironstone of Agbaja Plateau, Kabba Province. Record of Geological Survey Nigeria: pp. 20-43.

Jones, B. and Manning, D.A.C. (1994) . Comparison of geochemical indices used for the interpretation of palaeoredox conditions in ancient mudstones, Chemical Geology, 111 (1–4) , pp. 111–129.

Kandemir, R., Merve, O. and Orhan, K. (2022) . Sedimentological and geochemical characteristics of Lower Jurassic Sandstones from Gumushane, NE Turkey: implications for source to sink processes, paleoenvironmental conditions, provenance and tectonic settings. International Geology Review, 64 (12) , pp. 1719–1742

Kennedy, W.Q. (1965) . The influence of basement structure on the evolution of the coastal (Mesozoic and Tertiary) basins. In: Recent Basins Around Africa. Proceedings of the Institute of Petroleum Geologists Society, pp. 35–47

King, L.C. (1950) . Outline and distribution of Gondwanaland. Geological Magazine 87: 353–359.

Kogbe, C.A., Ajakaiye, D.E., Matheis, G. (1983) . Confirmation of rift structure along the Mid-Niger valley, Nigeria. Journal of African Earth Sciience, 1, pp.127–131.

Le Bas, M. J., Le Maitre, R. W.,Streckeisen, A. and Zanettin, B. (1986) . A chemical classification of volcanic rocks based on the total alkali-silica diagram. Journal of Petrology, 27, pp. 745–750.

Lezin, C., Andreu, B., Pellenard, P., Bouchez, J-L., Emmanuel, L., Faure, P. and Landrein, P. (2013) . Geochemical disturbance and paleoenvironmental changes during the Early Toarcian in NW Europe. Chemical Geology, 341, pp. 1–15

Li, D, Shi, Q. and Mi, N. (2020) . The type, origin and preservation of organic matter of the fine-grain sediments in Triassic Yanhe Profile, Ordos Basin, and their relation to paleoenvironment condition. Journal of Petroleum Science and Engineering, 188, pp. 106875

Liu, G. and Zhou, D.S. (2007) . Application of microelements analysis in identifying sedimentary environment–taking Qianjiang Formation in the Jiang Han Basin as an example. Petroleum Geology and Experiment, 29 (3) , pp. 307–311.

Liu, B., Huang, W.H., Ao, W. H., Yan, D. Y., Xu, Q. L. and Teng, J. (2015) . Geochemistry characteristics of rare earth elements in the late Paleozoic coal from Qinshui Basin. Journal of China Coal Society, 40, pp. 2916−2926.

McLennan, S.M. (1989) . Rare earth elements in sedimentary rocks; influence of provenance and sedimentary processes, in Lipin, B.R., McKay, G.A. (eds.) , Geochemistry and Mineralogy of Rare Earth Elements. Reviews in Mineralogy, 21, pp. 169-200.

McLennan, S.M., Hemming, S., McDaniel, D.K. and Hanson, G.N. (1993) . Geochemical approaches to sedimentation, provenance, and tectonics. Geological Society of America Special Papers, 284, pp. 21 - 40

Mebradu, S., Imhanobe, J. and Kpandei, L. Z. (1986) . Palynostratigraphy of the Ahoko sediments from the Nupe basin, N.W. Nigeria. Review of Palaeobotany and Palynology, 48, pp. 303-310

Nace, T.E., Baker, P.A., Dwyer, G.S., Silva, C.G., Rigsby, C.A. and Burns, S.J. (2014) . The Role of North Brazil Current Transport in the Paleoclimate of the Brazilian Nordeste Margin and Paleoceanography of the Western Tropical Atlantic During the Late Quaternary. Paleogeography. Palaeoclimatology. Palaeoecology., 415, pp. 3–13

Obaje, N.G. (2009) . Geology and Mineral Resources of Nigeria. Springer, p. 221

Ojo, O.J. and Akande, S.O. (2006) . Sedimentological and Palynological studies of the Patti Formation, south eastern Bida Basin, Nigeria: Implications for paleoenvironment and Paleogeography. NAPE Bulletin., 19, pp. 61-77.

Ojo, O.J. and Akande, S.O. (2008) . Microfloral assemblage, age and paleoenvironment of the Upper Cretaceous Patti Formation, southeastern Bida Basin, Nigeria. Journal of Mining and Geology, 44, pp. 71-78.

Ojo, O.J. (2010) . Occurrence of some Maastrichtian Dinoflagellate cysts from the Upper Cretaceous sediment of the Bida Basin, Nigeria: Implications for age and paleoenvironments. Global Journal of Geological Sciences, 8 (2) , pp. 217-230

Ojo, O.J. and Akande, S.O. (2009) . Sedimentology and depositional environments of the Maastrichtian Patti Formation, southeastern Bida Basin, Nigeria. Cretaceous Research, 30, pp. 1415-1425

Ojo, O.J. and Akande, S.O. (2012) . Sedimentary Facies Relationships and Depositional Environments of the Maastrichtian Enagi Formation, Northern Bida Basin, Nigeria. Journal of Geography and Geology, 4 (1) , pp. 136-147

Ojo, O.J., Adepoju, S.A. and Adedoyin, D.A. (2015) . Combined Petrographic and Geochemical Studies of Maastrichtian Patti Formation Sandstone, Bida Basin, Nigeria: Implications for Provenance and Compositional Maturity. Ilorin Journal of Science, 2 (1) , p. 163 – 189, https://doi.org/10.54908/iljs.2015.02.01.012

Ojo, O.J. and Akande, S.O. (2020) . A revised stratigraphy of the Bida Basin, Nigeria by Rahaman et al., (2019) [Journal of African Earth Science, 151, 67–81]: A rebuttal. Journal of African Earth Sciences, 172, pp. 1-14

Ojo, O.J., Jimoh, A.Y., Umelo, J.C. and Akande, S.O. (2020) . Organic geochemical and palynological studies of the Maastrichtian source rock intervals in Bida Basin, Nigeria: implications for hydrocarbon prospectivity. Journal of Petroleum Exploration and Production Technology, pp. 1-16

Ojo, O.J., Adepoju, S.A., Awe, A. and Adeoye, M. O. (2021) . Mineralogy and geochemistry of the sandstone facies of Campanian Lokoja formation in the Southern Bida basin, Nigeria: implications for provenance and weathering history. Heliyon, 7, pp. 1-12

Ojo, S.B. and Ajakaiye, D.E. (1989) . Preliminary Interpretation of Gravity Measurements in the Middle Niger Basin Area, Nigeria. In: Kogbe, C.A., Ed., Geology of Nigeria: 2nd Edition, Elizabethan Publishing Company, Lagos, pp. 347-358.

Omietimi, E.J., Lenhardt, N. and Yang, R. (2021) . Sedimentary geochemistry of Late Cretaceous-Paleocene deposits at the southwestern margin of the Anambra Basin (Nigeria) : Implications for paleoenvironmental reconstructions. Palaeogeography, Palaeoclimatology, Palaeoecology, 600 (12) , pp. 111059

Pehlivanli, B.Y. (2019) . Factors controlling the paleo-sedimentary conditions of Çeltek oil shale, Sorgun-Yozgat/Turkey. Bulletin of the Mineral Research and Exploration, 158, pp. 251–263.

Rahaman, M.A.O., Fadiya, S.L., Adekola, S.A., Coker, S.J., Bale, R.B., Olawoki, O.A., Omada, I.J., Obaje, N.G., Akinsanpe, O.T., Ojo, G.A., and Akande, W.G. (2019) . A revised stratigraphy of the Bida Basin, Nigeria. Journal of African Earth Sciences, 151, pp. 67 – 81

Rohl, H.J., Schmid-Rohl, A., Oschmann, W., Frimmel, A. and Schwark, L. (2001) . The Posidonia Shale (Lower Toarcian) of SW-Germany: an oxygen-depleted ecosystem controlled by sea-level and palaeoclimate. Paleogeography. Paleoclimatology. Paleoecology., 165 (1–2) , pp. 27–52

Roser, B.P. and Korsch, R.J. (1986) . Determination of tectonic setting of sand-stone mudstone suites using SiO2 content and K_2O/Na_2O ratio. Journal of Geology, 94, pp. 635-650.

Roser, B.P., Cooper, R.A., Nathan, S.A. and Tulloch, A. J. (1996) . Reconnaissance sandstone geochemistry, provenance, and tectonic setting of the lower Paleozoic terrains of the west coast and Nelson, New Zealand. New Zealand Journal of Geology and Geophysics., 39, pp. 1–16

Salawu, N.B, Dada, S.S., Fatoba, J.O., Ojo, O.J., Adebiyi, L.S., Sunday, A.J. and Abdulraheem, T. Y., 2021, Structural architecture of the Middle Niger Basin, Nigeria based on aeromagnetic data: An example of a non-volcanic basin: Heliyon, DOI:https://doi.org/10.1016/j.heliyon.2021.e07205

Sarki Yandoka, B.M., Abubakar, M.B., Abdullah, W.H., Maigari, A.S, Hakimi, M.H., Adegoke, A.K., Shirputda, J.J. and Aliyu, A.H. (2015) . Sedimentology, geochemistry and paleoenvironmental reconstruction of the Cretaceous Yolde Formation from Yola Sub-basin, Northern Benue Trough, NE Nigeria. Marine and Petroleum Geology, 65, pp 663 – 677, http://dx.doi.org/10.1016/j.marpetgeo.2015.06.009

Schoepfer, S.D., Shen, J., Wei, H., Tyson, R.V., Ingall, E. and Algeo, T.J. (2015) . Total organic carbon, organic phosphorus, and biogenic barium fluxes as proxies for paleomarine productivity. Earth-Sci Rev., 149, pp. 23–52

Scotese, C.R., Song, H., Mills, B.J. and van der Meer, D.G. (2021) . Phanerozoic paleotemperatures: The earth's changing climate during the last 540 million years. Earth-Science Reviews, 125, p. 1 – 126, https://doi.org/10.1016/j.earscirev.2021.103503

Skelton, P.W., Spicer, R.A., Kelley, S.P. and Gilmour, L. (2003) . The Cretaceous World: Cambridge University Press, Cambridge, pp. 360

Song, J., Zhao, X.M. and Chen, D.C. (2012) Rare earth and trace elements geochemical characteristics of the dark Permian mudstones in Ejinaqi and its surrounding areas, western inner Mongolia. Acta Geologica Sinica, 86 (11) , pp. 1773–1780.

Song, J., Bao, Z., Zhao, X., Gao, Y., Song, X., Zhu, Y., Deng, J., Liu, W., Wang, Z., Ming, C., Meng, Q., Zhang, L., Mao, S., Zhang, Y., Yu, X. and Wei, M. (2018) . Sedimentology and geochemistry of Middle–Upper Permian in northwestern Turpan–Hami Basin, China: Implication for depositional environments and petroleum geology. Energy Exploration and Exploitation, 36 (4) , pp. 910–941

Sousa, T.A., Venancio, I.M., Marques, E.D., Figueiredo, T.S., Nascimento, R.A., Smoak, J.M., Albuquerque, A.L.S., Valeriano, C. M. and Silva-Filho, E. V. (2022) . REE Anomalies Changes in Bottom Sediments Applied in the Western Equatorial Atlantic Since the Last Interglacial. Frontier Marine Science., 9 (8) , pp. 1-14

Suttner, L.J. and Dutta, P.K. (1986) . Alluvial sandstone composition and paleoclimate, I. Framework mineralogy. Journal of Sedimentary Petrology, 56 (3) , pp. 329-345

Taylor, S.R. and McLennan, S. (1985) . The Continental Crust: Its Composition and Evolution: Blackwell Scientific Publication Palo Alto, CA, U.S.A., pp. 328

Teng, G.E. (2004) . The Distribution of elements, carbon and oxygen isotopes on marine strata and environmental correlation between them and hydrocarbon source rocks formation - An example from Ordovician Basin, China. PhD Dissertation. Graduate School of Chinese Academy of Sciences (Lanzhou Institute of Geology) , Lanzhou (in Chinese) .

Tribovillard, N., Algeo, T.J., Lyons, T., and Riboulleau, A. (2006) . Trace Metals as Paleoredox and Paleoproductivity Proxies: An Update. Chemical Geology, 232 (2) , pp. 12–32

Trueman, C.N. and Tuross, N. (2002) . Trace elements in recent and fossil bone apatite. Reviews in Mineralogy and Geochemistry, 48 (1) , pp. 489–521.

Udensi, E.E. and Osazuwa, I.B. (2004) . Spectra determination of depths to magnetic rocks under the Nupe basin, Nigeria. Nigeria Association of Petroleum Explorationists (NAPE) Bulletin, 17,pp. 22–27.

Venancio, I.M., Mulitza, S., Govin, A., Santos, T.P., Lessa, D.O. and Albuquerque, A. (2018) . Millennial-to Orbital-Scale Responses of Western Equatorial Atlantic Thermocline Depth to Changes in the Trade Wind System Since the Last Interglacial. Paleoceanography. Paleoclimatology, 33 (12) , pp. 1490–1507

Waelbroeck, C., Labeyrie, L., Michel, E., Duplessy, J.C., Mcmanus, J.F. and Lambeck, K. (2002) . Sea-level and Deep-Water Temperature Changes Derived From Benthic Foraminifera Isotopic Records. Quaternary Science Review, 21 (1-3) , pp. 295–305

Wang, Z.G., Yu, X.Y. and Zhao, Z.H. (1989) . Geochemistry of Rare Earth Elements. Science Press Beijing, 1989; pp 279−289.

Wang, J.S., Huang, X.Z., Sui, J.C., Shao, H.S., Yan, C.F., Wang, S.Q. and He, Z.R. (1997) . Evolutional characteristics and their paleoclimate significance of trace elements in the Hetaoyuan Formation, Biyang depression. Acta Sedimentological Sinica., 15, pp. 65–70.

Wang, J.B., He, Z.L. and Zhu, D.Y. (2020) . Geochemical characteristics, depositional environment, and provenance attitude of the Middle Jurassic Yangye Formation lacustrine mudstones in Kashi Sag, south‐western Tarim Basin." Geological Journal, 55 (4) , pp. 2976–2994.

Wei, W., and Algeo, T.J. (2020) . Elemental proxies for paleosalinity analysis of ancient shales and mudrocks. Geochimica et Cosmochimica Acta, 287, pp. 341–366

Wei, G.J., Liu, Y., Li, X.H., Liang, X.R. and Shao, L. (2003) . Excess Al in the sediments from South China Sea. Bulletin of Mineralogy Petrology and Geochemistry, 22 (1) , pp. 23–25

Werne, J.P., Sageman, B.B., Lyons, T.W. and Hollander, D.J. (2002) . An integrated assessment of a "type euxinic" deposit: evidence for multiple controls on black shale deposition in the Middle Devonian Oatka Creek Formation. American Journal of Science, 302 (2) , pp. 110–143..

Xu, Z., Lu, H., Zhao, C., Wang, X., Su, Z., Wang, Z., Liu, H., Wang, L., Lu, Q. (2010) . Composition, origin and weathering process of surface sediment in Kumtagh Desert, Northwest China. Journal of Geographical Science 21, 1062–1076.

Yu, C., Huang, W., Jiu, B. and Hao, R. (2022) . Geochemistry Characteristics and Paleoenvironmental Significance of Trace Elements in Coal and Coal Gangue in the Yangcheng Mining Area, Qinshui Basin. American Chemical Society Omega, 7, pp. 13557−13576

Zhang, J, Wang, C. and Wang, J. (2021) . Paleoclimate of the Paleogene Dongying formation in Bozhong Sag of Bohai Bay Basin. Petroleum Research, 6, 368 – 378 , https://doi.org/10.1016/j.ptlrs.2021.04.002

Zhao, Y., Liu, C.Y., Niu, H.Q., Zhao, X.C., Zhang, D.D., Yang, D. and Hui, D. (2017) . Trace and rare earth element geochemistry of crude oils and their coexisting water from the Jiyuan Area of the Ordos Basin, N China: Geological Journal, 53, pp. 336-348.

Zou, S., C., Wu, D., Xu, Q., Shan, X., Zhang, and P., Hollings, 2016, Provenance and depositional setting of lower Silurian siliciclastic rocks on Hainan Island, south China: implications for a passive margin environment of south China in Gondwana: J. Asian Earth Sci., v. 123, p. 243 - 262

GARNET ENERGY SERVICES NIGERIA LTD.

Geological, Petroleum and Environmental Consultants

12 Floor, Bookshop House, 50/52 Broad Street, Lagos
P.O. Box 70011, Victoria Island, Lagos, Nigeria
Tel. 01-8546699, 08035101804
E-mail mariesonuga@yahoo.com

BARACAL CONSULT LTD.

Environmental Consultants

Suite 65/66 Dolphin Plaza, Dolphin Estate, Ikoyi
P.O. Box 70885, Victoria Island, Lagos, Nigeria
Tel. 234-1-7741441, 234-1-2629251 *Fax* 234-1-2610735
E-mail baracalnig@yahoo.com, carolsoladg@yahoo.com

Jonakod

Jonakod Nigeria Limited

Energy, Environment & Safety Consultants

34 Ontario Crescent, Maitama, Abuja
Tel. 09-4133521, 08035300958, 08057467878
E-mail jonas.odocha@yahoo.com

AMJU SERVICES NIG. LTD.

Specialists in Geological & Mining Services

1B Rock Road, Off Rabah Road
P.O. Box 7216, Kaduna, Nigeria
Tel. +234-(0)8054073338
E-mail abuykarofi@gmail.com